

See discussions, stats, and author profiles for this publication at: <https://www.researchgate.net/publication/8988638>

Sidewall Functionalization of Single-Walled Carbon Nanotubes by Addition of Dichlorocarbene

ARTICLE *in* JOURNAL OF THE AMERICAN CHEMICAL SOCIETY · JANUARY 2004

Impact Factor: 12.11 · DOI: 10.1021/ja0356737 · Source: PubMed

CITATIONS

281

READS

47

6 AUTHORS, INCLUDING:



Katalin Kamaras

Hungarian Academy of Sciences

178 PUBLICATIONS 4,726 CITATIONS

SEE PROFILE

Sidewall Functionalization of Single-Walled Carbon Nanotubes by Addition of Dichlorocarbene

Hui Hu, Bin Zhao, Mark A. Hamon, Katalin Kamaras,[†] Mikhail E. Itkis, and Robert C. Haddon*

Contribution from the Center for Nanoscale Science and Engineering,
Departments of Chemistry and Chemical & Environmental Engineering,
University of California, Riverside, California 92521-0403

Received April 16, 2003; E-mail: haddon@ucr.edu

Abstract: We report the sidewall functionalization of soluble HiPco single-walled carbon nanotubes (SWNTs) by addition of dichlorocarbene. The dichlorocarbene-functionalized SWNTs [(s-SWNT)CCl₂] retain their solubility in organic solvents such as tetrahydrofuran and dichlorobenzene. The degree of dichlorocarbene functionalization was varied between 12% and 23% by using different amounts of the dichlorocarbene precursor. Because the addition of dichlorocarbene saturates the carbon atoms on the sidewall of the SWNTs and effectively replaces the delocalized partial double bonds with a cyclopropane functionality, the optical spectra of the SWNTs change dramatically. We estimate that the saturation of 25% of the π -network electronic structure of the SWNTs is sufficient to remove all vestiges of the interband transitions in the infrared spectrum. The transitions at the Fermi level in the metallic SWNTs that appear in the far-infrared (FIR) region of the spectrum show a dramatic decrease of intensity on dichlorocarbene functionalization. The FIR region of the spectrum allows a clear differentiation between the covalent and the ionic chemistry of SWNTs. In contrast with covalent functionalization, we show that reaction of the SWNTs with bromine vapor leads to a strong increase in absorptions at the Fermi level that is observable in the FIR due to hole doping of the semiconducting SWNTs. Thermal treatment of the (s-SWNT)CCl₂ above 300 °C resulted in the breakage of C–Cl bonds, but did not restore the original electronic structure of the SWNTs.

Introduction

Chemical functionalization of the sidewalls of single-walled carbon nanotubes (SWNTs) has attracted interest because this is a promising way to improve the solubility of the SWNTs and to facilitate their manipulation. A number of sidewall derivatization schemes have been developed, using nitrenes, Birch reduction conditions, dichlorocarbene,^{1,2} and fluorine.³ SWNTs with alkyl substituents have been obtained by treating the fluorinated SWNTs with nucleophilic reagents such as alkyllithium and alkylmagnesium bromides.^{4,5} The sidewall derivatization of SWNTs has been achieved by the generation of alkyl radicals,⁶ aryl radicals,^{7–9} azomethine ylides,¹⁰ and

carbenes.^{1,2,11} Several methods for the metal reduction of SWNTs have also been reported.^{1,12} The functionalization methodology of most of these processes is based on the reaction of electrophilic reagents with the partial carbon–carbon double bonds in the sidewall of the SWNTs.

Soluble SWNTs (s-SWNT) in amide form are particularly advantageous because they allow organic solution-phase chemistry.^{2,13,14} Thus, it is possible to affect some purification of the reaction products and to carry out analytical studies of the functionalized material. We have reported the addition of dichlorocarbene to the sidewalls of both insoluble SWNTs¹ and shortened s-SWNTs.² In the latter case, we utilized SWNTs produced in the electric arc (EA) process, and solution-phase near-infrared (NIR) spectroscopy of the dichlorocarbene-functionalized soluble SWNTs [(s-SWNT)CCl₂] was used to monitor the sidewall chemistry. This was the first report of the use of solution-phase NIR to follow the evolution of the electronic structure of the SWNTs as a result of covalent and ionic

[†] Permanent address: MTA SzFKI, Budapest, Hungary.

- (1) Chen, Y.; Haddon, R. C.; Fang, S.; Rao, A. M.; Eklund, P. C.; Lee, W. H.; Dickey, E. C.; Grulke, E. A.; Pendergrass, J. C.; Chavan, A.; Haley, B. E.; Smalley, R. E. *J. Mater. Res.* **1998**, *13*, 2423–2431.
- (2) Chen, J.; Hamon, M. A.; Hu, H.; Chen, Y.; Rao, A. M.; Eklund, P. C.; Haddon, R. C. *Science* **1998**, *282*, 95–98.
- (3) Mickelson, E. T.; Huffman, C. B.; Rinzler, A. G.; Smalley, R. E.; Hauge, R. H.; Margrave, J. L. *Chem. Phys. Lett.* **1998**, *296*, 188–194.
- (4) Boul, P. J.; Liu, J.; Mickelson, E. T.; Huffman, C. B.; Ericson, L. M.; Chiang, I. W.; Smith, K. A.; Colbert, D. T.; Hauge, R. H.; Margrave, J. L.; Smalley, R. E. *Chem. Phys. Lett.* **1999**, *310*, 367–372.
- (5) Saini, R. K.; Chiang, I. W.; Peng, H.; Smalley, R. E.; Billups, W. E.; Hauge, R. H.; Margrave, J. T. *J. Am. Chem. Soc.* **2003**, *125*, 3617–3621.
- (6) Ying, Y.; Saini, R. K.; Liang, F.; Sadana, A. K.; Billups, W. E. *Org. Lett.* **2003**, *5*, 1471–1473.
- (7) Bahr, J. L.; Yang, J.; Kosynkin, D. V.; Bronikowski, M. J.; Smalley, R. E.; Tour, J. M. *J. Am. Chem. Soc.* **2001**, *123*, 6536–6542.
- (8) Bahr, J. L.; Tour, J. L. *Chem. Mater.* **2001**, *13*, 3823–3824.
- (9) Dyke, C. A.; Tour, J. M. *J. Am. Chem. Soc.* **2003**, *125*, 1156–1157.

- (10) Georgakilas, V.; Kordatos, K.; Prato, M.; Guldi, D. M.; Holzinger, M.; Hirsch, A. *J. Am. Chem. Soc.* **2002**, *124*, 760–761.
- (11) Holzinger, M.; Vostrowsky, O.; Hirsch, A.; Hennrich, F.; Kappes, M.; Weiss, R.; Jellen, F. *Angew. Chem., Int. Ed.* **2001**, *40*, 4002–4005.
- (12) Pekker, S.; Salvétat, J.-P.; E., J.; Bonard, J.-M.; Forro, L. *J. Phys. Chem. B* **2001**, *105*, 7938–7943.
- (13) Hamon, M. A.; Chen, J.; Hu, H.; Chen, Y.; Rao, A. M.; Eklund, P. C.; Haddon, R. C. *Adv. Mater.* **1999**, *11*, 834–840.
- (14) Chen, J.; Rao, A. M.; Lyuksyutov, S.; Itkis, M. E.; Hamon, M. A.; Hu, H.; Cohn, R. W.; Eklund, P. W.; Colbert, D. T.; Smalley, R. E.; Haddon, R. C. *J. Phys. Chem. B* **2001**, *105*, 2525–2528.

functionalization, and since that time this has become the preferred analytical tool for the demonstration of carbon nanotube wall chemistry. Although the addition of dihalocarbenes to fullerenes is well documented,^{15–17} theoretical studies have raised questions about the viability of binding dichlorocarbene to the sidewalls of carbon nanotubes.¹⁸

To address these questions and to fully document the addition of dichlorocarbene to the sidewalls of carbon nanotubes, we report a systematic study of dichlorocarbene addition to HiPco s-SWNT. We also report the reaction of the SWNTs with bromine vapor, to contrast the far-infrared (FIR) spectral response that is observed on carrying out covalent and ionic chemistry on SWNTs. The HiPco SWNTs are of a smaller diameter^{19,20} and are therefore expected to exhibit a higher reactivity^{1,21,22} in sidewall addition reactions than the EA material that was previously studied.² In addition, the HiPco SWNTs are of higher purity^{19,23} than the EA SWNTs, and the identification of the reaction products is expected to be more definitive.²⁴ We also report the effect of thermal treatment on the optical properties of dichlorocarbene-functionalized SWNT films.

Experimental Section

As-prepared (AP) HiPco SWNTs were purchased from Carbon Nanotechnologies Inc. The dichlorocarbene precursor $\text{PhHgCCl}_2\text{Br}$ was synthesized according to literature procedures.²⁵ All other chemical reagents were purchased from Aldrich and used as received. A sample of dichlorocarbene-functionalized C_{70} was provided by Dr. M. Meier, Department of Chemistry, University of Kentucky, for mid-IR characterization. Atomic force microscopy (AFM) images were obtained with a Digital Instruments Nanoscope IIIA, in tapping mode. Spectra were obtained on a Bruker RFS 100/s spectrometer (Raman), a Cary 500 scan UV–vis–IR spectrometer (vis–NIR), a Nicolet Magna-IR 560 E.S.P. spectrometer (NIR and mid-IR), and a Bruker IFS-120HR FT-IR spectrophotometer (mid-IR and FIR). Semitransparent films for the spectral measurements were prepared by spraying SWNT dispersion in organic solvents on the heated optical substrates (sapphire or silicon).

Preparation of Soluble Amide HiPco SWNTs [s-SWNT (1)]. The purification of the HiPco SWNTs followed literature methods.²⁰ After purification, HiPco SWNTs (100 mg) were refluxed in 100 mL of 2–3 M nitric acid for 24 h to introduce carboxylic acid groups.^{26,27} The SWNT–COOH product (50 mg) was dispersed in 50 mL of dimethylformamide (DMF) by a 15-min sonication treatment. Next, 2 mL of

oxalyl chloride was added dropwise to the dispersion of SWNTs at 0 °C under argon, and the mixture was stirred at 0 °C for 2 h and then at room temperature for a further 2 h. The excess oxalyl chloride was removed by heating the reaction mixture at 70 °C for 16 h. The SWNTs in acyl chloride form (SWNT–COCl) were collected by filtration through a membrane (pore size 0.2 μm) and dried under vacuum. SWNT–COCl (50 mg) was heated with 500 mg of octadecylamine (ODA) at 100 °C for 5 days. After being washed with ethanol to remove the excess ODA, the black solid was treated with THF. The black mixture was then filtered through a coarse filter paper, and the black filtrate was taken to dryness on a rotary evaporator (final weight of s-SWNT (1): 60 mg).

End-Group Analysis of s-SWNT (1). s-SWNT (1) (0.69 mg) was dissolved in 1.38 mL of tetrachlorocarbon. The mid-IR spectrum of s-SWNT (1) in DMF solution was measured on a Nicolet Magna-IR 560 E.S.P. spectrometer, and the absorbance intensity of the symmetric $\nu(\text{C–H})$ stretch was found to be 0.048. By using the end-group analysis method,^{28,29} the molar percentage of ODA in s-SWNT (1) was determined as 4%.

Dichlorocarbene Addition to s-SWNT: Preparation of (s-SWNT) CCl_2 (2). In a typical reaction, s-SWNT (1) (20 mg) and $\text{PhHgCCl}_2\text{Br}$ (1 g) were dissolved in dichlorobenzene. The reaction mixture was stirred at 85 °C under argon for 48 h. The mixture was filtered through a coarse filter paper to remove the resulting precipitate of PhHgBr . The black-colored filtrate was concentrated on a rotary evaporator and added to acetone. The precipitate was collected via filtration and dried at room temperature under vacuum; the final weight of (s-SWNT) CCl_2 (2b) was 6 mg.

Doping of a s-SWNT Film with Bromine Vapor. The s-SWNT films on optical substrates were placed in a closed container in the presence of bromine for 1 h.

Results and Discussion

Analysis of Soluble SWNTs and Dichlorocarbene Reaction Products. The SWNT dissolution and dichlorocarbene addition reactions are illustrated in Scheme 1. The nitric-acid-treated SWNTs were functionalized with carboxylic acid groups. The amidation of the carboxylic acid form of the SWNTs with octadecylamine (ODA) was carried out via an acyl chloride intermediate. End-group analysis showed that about 4 atom % of the carbon atoms were functionalized with ODA. A series of dichlorocarbene addition reactions was carried out with different amounts of $\text{PhHgCCl}_2\text{Br}$ to give dichlorocarbene-derivatized soluble SWNTs [(s-SWNT) CCl_2 (2a–c)] (Table 1), which retained their solubility in organic solvents such as tetrahydrofuran and dichlorobenzene. Energy-dispersive X-ray spectroscopy (EDS) of the (s-SWNT) CCl_2 (2a–c) showed that the atomic percentage of chlorine in the products varied from 8% to 14% (Table 1). To estimate the degree of functionalization, we assumed that the atomic percentage of carbon (C%) obtained in the EDS analysis originated from both the tube sidewall ($\text{C}_{\text{wall}}\%$) and the dichlorocarbene adducts ($\text{C}_{\text{add}}\%$). $\text{C}_{\text{add}}\%$ is equal to $1/2\text{Cl}\%$, and $\text{C}_{\text{wall}}\%$ can be calculated from

$$\text{C}_{\text{wall}}\% = (\text{C}\% - \text{C}_{\text{add}}\%) = (\text{C}\% - 1/2\text{Cl}\%)$$

and the degree of dichlorocarbene functionalization is given by $(\text{Cl}/\text{C}_{\text{wall}})\%$ (Table 1).

Figure 1a and 1b shows the AFM images of soluble amide HiPco SWNTs [s-SWNT (1)] and (s-SWNT) CCl_2 (2b) on a

- (15) Tsuda, M.; Ishida, T.; Nogami, T.; Kurono, S.; Ohashi, M. *Tetrahedron Lett.* **1993**, *34*, 6911–6912.
- (16) Osterodt, J.; Vogtle, F. *Chem. Commun.* **1996**, 547–548.
- (17) Kiely, A. F.; Haddon, R. C.; Meier, M. S.; Selegue, J. P.; Brock, C. P.; Patrick, B. O.; Wang, G. W.; Chen, Y. *J. Am. Chem. Soc.* **1999**, *121*, 7971–7972.
- (18) Jaffe, R. L. *Proc. Electrochem. Soc.* **1999**, *12*, 153–162.
- (19) Nikolaev, P.; Bronikowski, M. J.; Bradley, R. K.; Rohmund, F.; Colbert, D. T.; Smith, K. A.; Smalley, R. E. *Chem. Phys. Lett.* **1999**, *313*, 91–97.
- (20) Zhou, W.; Ooi, Y. H.; Russo, R.; Papanek, P.; Luzzi, D. E.; Fischer, J. E.; Bronikowski, M. J.; Willis, P. A.; Smalley, R. E. *Chem. Phys. Lett.* **2001**, *350*, 6–14.
- (21) Haddon, R. C. *Science* **1993**, *261*, 1545–1550.
- (22) Niyogi, S.; Hamon, M. A.; Hu, H.; Zhao, B.; Bhowmik, P.; Sen, R.; Itkis, M. E.; Haddon, R. C. *Acc. Chem. Res.* **2002**, *35*, 1105–1113.
- (23) Chiang, I. W.; Brinson, B. E.; Huang, A. Y.; Willis, P. A.; Bronikowski, M. J.; Margrave, J. L.; Smalley, R. E.; Hauge, R. H. *J. Phys. Chem. B* **2001**, *105*, 8297–8301.
- (24) Bettinger, H. F.; Kudin, K. N.; Scuseria, G. E. *J. Am. Chem. Soc.* **2001**, *123*, 12849–12856.
- (25) Seyferth, D.; Burlitch, J. M. *J. Organomet. Chem.* **1965**, *4*, 127–137.
- (26) Liu, J.; Rinzler, A. G.; Dai, H.; Hafner, J. H.; Bradley, R. K.; Boul, P. J.; Lu, A.; Iverson, T.; Shelimov, K.; Huffman, C. B.; Rodriguez-Macias, F.; Shon, Y.-S.; Lee, T. R.; Colbert, D. T.; Smalley, R. E. *Science* **1998**, *280*, 1253–1255.
- (27) Hu, H.; Bhowmik, P.; Zhao, B.; Hamon, M. A.; Itkis, M. E.; Haddon, R. C. *Chem. Phys. Lett.* **2001**, *345*, 25–28.

- (28) Hamon, M. A.; Hu, H.; Bhowmik, P.; Niyogi, S.; Zhao, B.; Itkis, M. E.; Haddon, R. C. *Chem. Phys. Lett.* **2001**, *347*, 8–12.
- (29) Hamon, M. A.; Hu, H.; Bhowmik, P.; Itkis, M. E.; Haddon, R. C. *Appl. Phys. A* **2002**, *74*, 333–338.

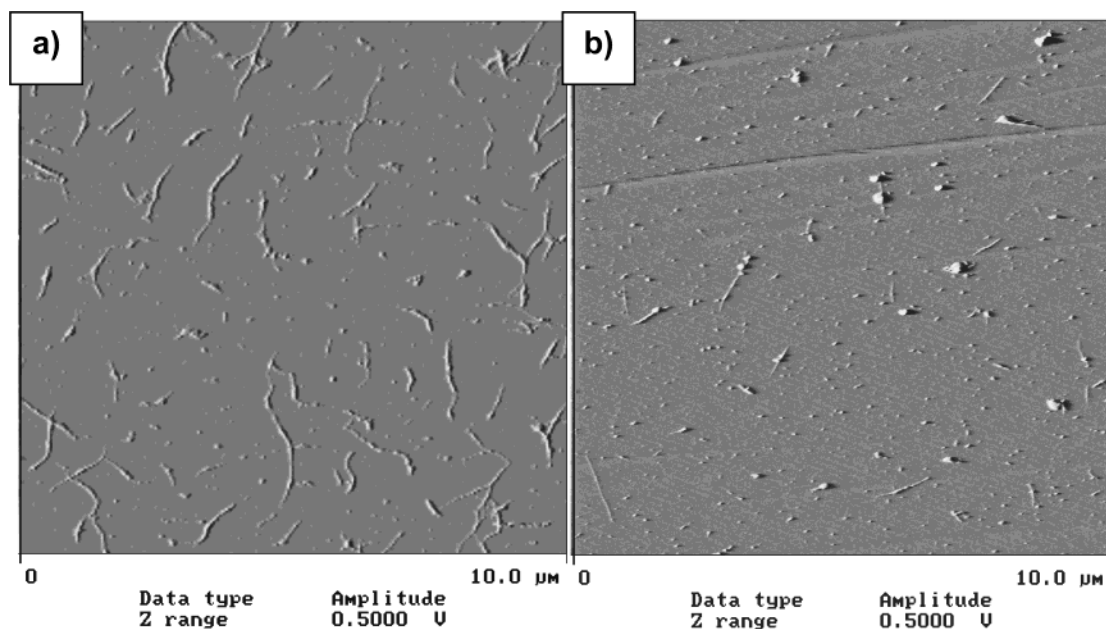
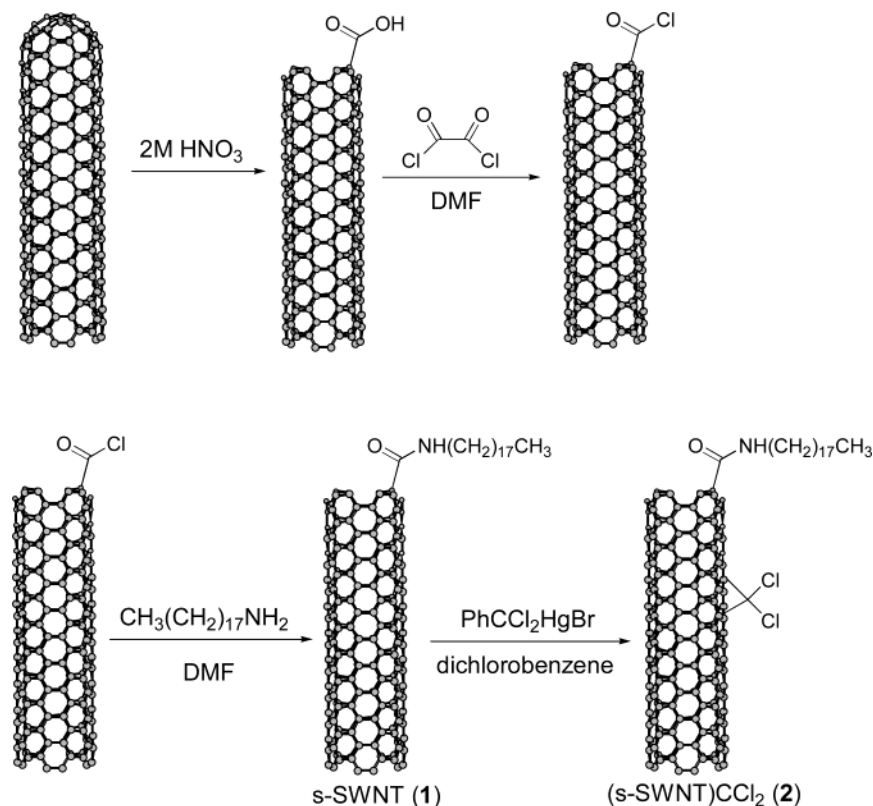


Figure 1. AFM images (mica substrate, from THF solution): (a) s-SWNT (**1**); (b) (s-SWNT)CCl₂ (**2b**).

Scheme 1. Dissolution and Dichlorocarbene Reaction of SWNTs



mica substrate. The average bundle sizes of s-SWNT (**1**) and (s-SWNT)CCl₂ (**2b**) are 2.7 and 2.0 nm, respectively, which indicates that the dichlorocarbene addition to the s-SWNT leads to a further defoliation of the nanotube bundles; this point is significant because the addition of substantial amounts of dichlorocarbene is expected to increase the effective diameter of the SWNTs.

Mid-IR Spectroscopy of SWNT Dichlorocarbene Reaction Products. Mid-IR spectra of s-SWNT (**1**) and (s-SWNT)CCl₂ (**2b**) are shown in Figure 2; the peak at 798 cm⁻¹ in the spectrum

of (s-SWNT)CCl₂ (**2b**) (Figure 2) is assigned to the C–Cl stretch and was previously observed to occur at the same frequency in the dichlorocarbene addition product of shortened, soluble EA SWNTs.² We found that the C–Cl stretch of dichlorocarbene-functionalized C₇₀¹⁷ occurs at 791 and 772 cm⁻¹.

Raman Spectroscopy of SWNT Dichlorocarbene Reaction Products. Raman spectroscopy is a useful tool for the characterization of SWNTs.^{20,30} The Raman spectrum of HiPco s-SWNT (**1**) (Figure 3a) displays two bands: the radial mode

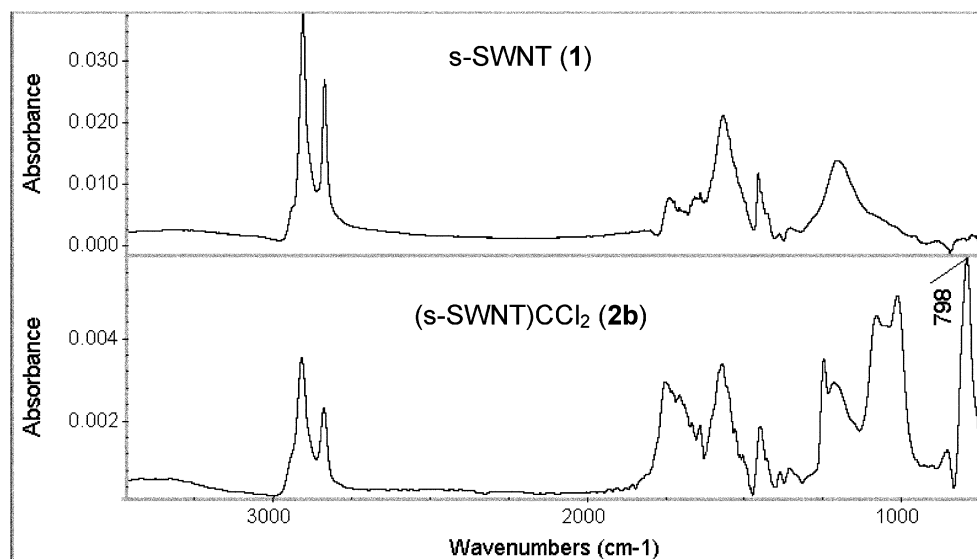


Figure 2. Mid-IR spectra (ATR method, after baseline correction) of s-SWNT (**1**) and (s-SWNT)CCl₂ (**2b**).

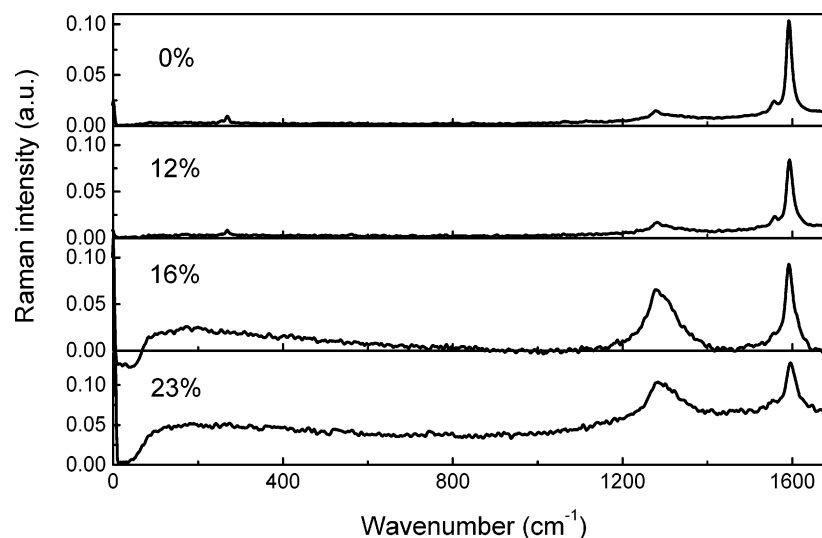


Figure 3. Raman spectra (film on Zn–Se substrate) of s-SWNT (**1**) (0%); (s-SWNT)CCl₂ (**2a**) (12%); (s-SWNT)CCl₂ (**2b**) (16%); (s-SWNT)CCl₂ (**2c**) (23%). The spectra are labeled with the degree of functionality (Cl/C_{wall})%.

Table 1. NIR Absorbance as a Function of the Degree of Dichlorocarbene Functionalization

sample	s-SWNT/PhHgCCl ₂ Br (weight ratio)	Cl (at. %)	degree of functionalization ^a	absorbances ^b	AA(S,X)/AA(T,X)	normalized absorption ratio ^c
s-SWNT (1)		0	0	0.21	0.083	1.00
(s-SWNT)CCl ₂ (2a)	1:8	8	12	0.14	0.061	0.73
(s-SWNT)CCl ₂ (2b)	1:50	11	16	0.05	0.018	0.22
(s-SWNT)CCl ₂ (2c)	1:100	14	23	0.04	0.009	0.11

^a Obtained from (Cl/C_{wall})% (see text). ^b The NIR absorbance is measured at 7000 cm^{−1}, with normalization at 8910 cm^{−1}. ^c Normalized absorption ratio = [AA(S, X)/AA(T, X)]/[AA(S, **1**)/AA(T, **1**)]. Areal absorptions (AA) obtained with spectral cutoffs of SCL = 5400 and SCH = 10 750 cm^{−1}.

($\omega_r = 267$ cm^{−1}) and the tangential mode ($\omega_t = 1595$ cm^{−1}). The weak band centered at 1285 cm^{−1} (ω_d) is attributed to disorder or the presence of sp³ hybridized carbon atoms in the benzenoid framework of the carbon nanotube walls. The Raman spectra of the (s-SWNT)CCl₂ (**2**) show that the intensity of the disorder mode grows at the expense of the radial and tangential modes (Figure 3), with an increasing degree of dichlorocarbene

functionalization in the (s-SWNT)CCl₂ (**2**). In the Raman spectra of samples **2b** and **2c**, the radial mode has almost completely disappeared.

Vis–NIR Spectroscopy of SWNT Dichlorocarbene Reaction Products. The vis–NIR spectra of s-SWNT (**1**) and (s-SWNT)CCl₂ (**2**) in dichlorobenzene are shown in Figure 4. The absorptions centered at 7000 cm^{−1} (0.90 eV), 12 150 cm^{−1} (1.50 eV), and 16 500 cm^{−1} (2.04 eV) have been previously observed in the spectra of HiPco SWNT³⁰ and are due to transitions between the first and second pairs of singularities in the density

(30) Hamon, M. A.; Itkis, M. E.; Niyogi, S.; Alvaraez, T.; Kuper, C.; Menon, M.; Haddon, R. C. *J. Am. Chem. Soc.* **2001**, *123*, 11292–11293.

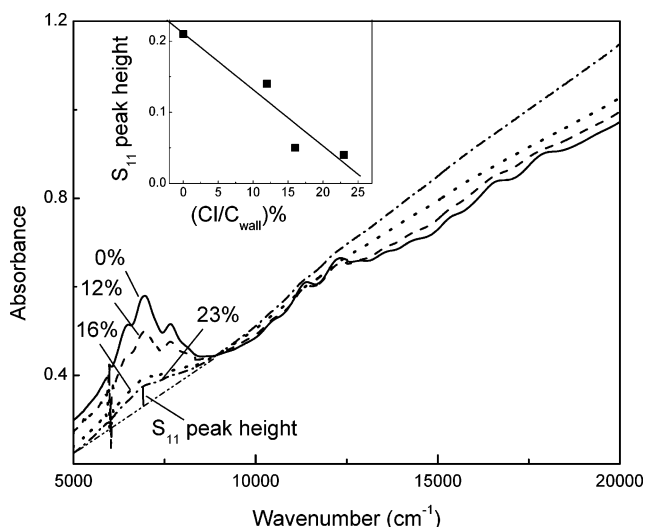


Figure 4. Solution-phase NIR spectra (dichlorobenzene, 0.125 mg/mL, quartz cell, light path 1 cm) of s-SWNT (**1**) (0%); (s-SWNT) CCl₂ (**2a**) (12%); (s-SWNT) CCl₂ (**2b**) (16%); (s-SWNT) CCl₂ (**2c**) (23%). The spectra are labeled with the degree of functionality (Cl/C_{wall})%. The spectra are normalized at 8910 cm⁻¹ (1.1 eV). The inset shows the S₁₁ peak height at 7000 cm⁻¹ versus (Cl/C_{wall})%.

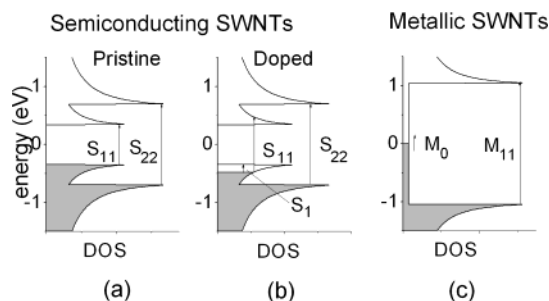


Figure 5. Schematic representation of the electronic density of states (DOS) of SWNTs that are responsible for transitions occurring in the NIR and FIR regions of the spectrum. (a) Pristine semiconducting SWNTs, where S₁₁ and S₂₂ correspond to the first and second interband transitions in the NIR spectral range. (b) Hole-doped semiconducting SWNTs, where intraband transitions involving free carriers (S₁) contribute to the FIR absorption. (c) Metallic SWNT, where M₁₁ is the first metallic band gap transition in the NIR range, and M₀ is the FIR transition due to intrinsically metallic SWNTs.

of states (DOS) of the semiconducting SWNTs (S₁₁ and S₂₂) and the first pair of singularities in the DOS of the metallic SWNTs (M₁₁), respectively.^{2,23,30–32} The interband electronic transitions provide characteristic signatures for the SWNTs,³³ and they are readily understood in terms of the electronic density of states (DOS) profile shown in Figure 5.

The spectra of (s-SWNT)CCl₂ (**2**) (Figure 4) show that the intensities of both the semiconducting (0.90 and 1.50 eV) and metallic transitions (2.04 eV) decrease with an increasing degree of dichlorocarbene functionalization. The fine structure in the absorptions of the (s-SWNT)CCl₂ (**2b**) and (**2c**) is indistinct as compared to that of s-SWNT starting material. This is because the sidewall functionalization destroys the extended π -network, thereby disrupting the translational symmetry and changing the

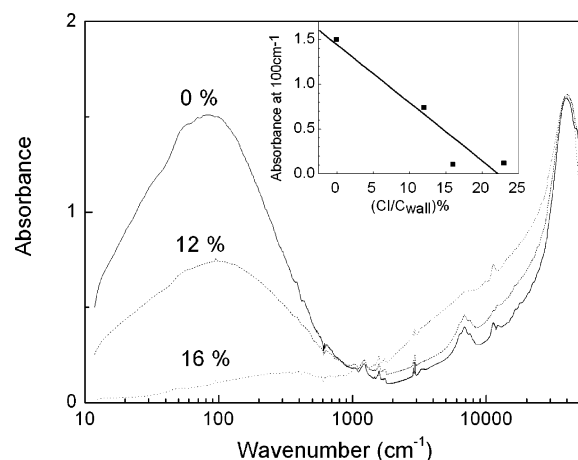


Figure 6. IR-vis-UV spectra of the films of s-SWNT (**1**) (0%); (s-SWNT)CCl₂ (**2a**) (12%); (s-SWNT)CCl₂ (**2b**) (16%). The spectra are labeled with the degree of functionality (Cl/C_{wall})% and are normalized at the π -plasmon peak (37 000 cm⁻¹). The inset shows the absorption height at 100 cm⁻¹ versus (Cl/C_{wall})%.

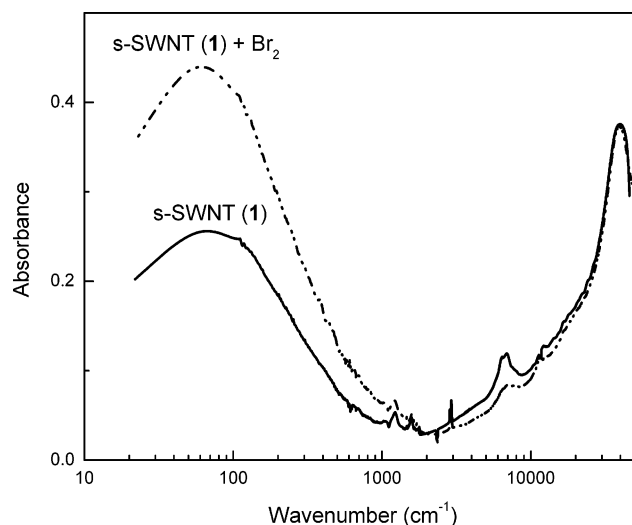


Figure 7. IR-vis-UV spectra of films of pristine s-SWNT (**1**), and after treatment with bromine vapor. The spectra are normalized at the π -plasmon peak (37 000 cm⁻¹).

electronic structure of the SWNTs, as previously observed for EA SWNTs.² These interband transitions are highly characteristic of the SWNTs and are a sensitive indicator of the integrity of the SWNT electronic structure; their diminution provides an ideal monitor for the introduction of substituents into the sidewalls of the SWNTs which function as defect sites in the SWNT electronic structure.^{34,35}

Quantitative NIR Analysis of SWNT Dichlorocarbene Reaction Products. Recently, we reported a method to evaluate the purity of EA AP-SWNT soot by using solution-phase NIR spectroscopy, in which the SWNT purity was evaluated against a reference sample by using the region of the second interband transition (S₂₂, with spectral cutoffs of SCL = 7750 and SCH = 11 750 cm⁻¹) for semiconducting SWNTs.³³ In the present paper, we use the region of the first interband transition (S₁₁, with spectral cutoffs of SCL = 5400 and SCH = 10 750 cm⁻¹)

- (31) Itkis, M. E.; Niyogi, S.; Meng, M.; Hamon, M.; Hu, H.; Haddon, R. C. *Nano Lett.* **2002**, *2*, 155–159.
 (32) Bachilo, S. M.; Strano, M. S.; Kittrell, C.; Hauge, R. H.; Smalley, R. E.; Weisman, R. B. *Science* **2002**, *298*, 2361–2366.
 (33) Itkis, M. E.; Perea, D.; Niyogi, S.; Rickard, S.; Hamon, M.; Hu, H.; Zhao, B.; Haddon, R. C. *Nano Lett.* **2003**, *3*, 309–314.

- (34) Crespi, V. H.; Cohen, M. L.; Rubio, A. *Phys. Rev. Lett.* **1997**, *79*, 2093–2096.
 (35) Charlier, J.-C. *Acc. Chem. Res.* **2002**, *35*, 1063–1069.

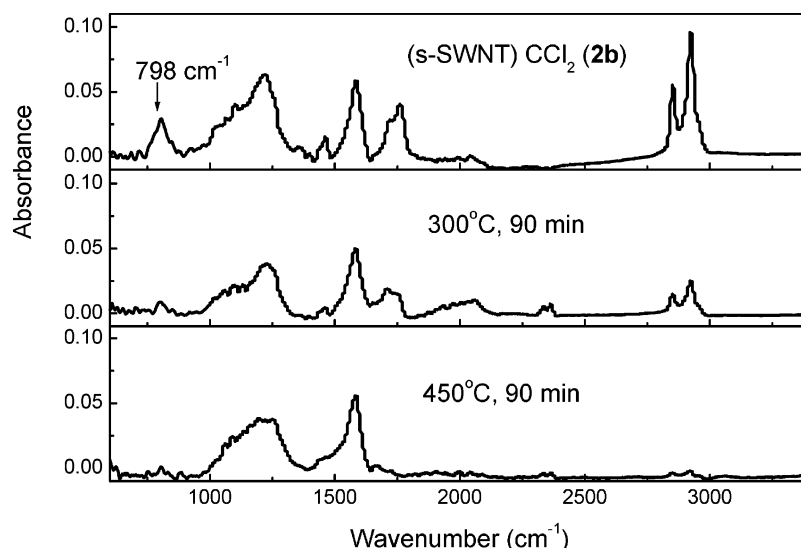


Figure 8. Mid-IR spectra (film on Zn–Se substrate, after baseline correction) of (s-SWNT)CCl₂ (**2b**) and (s-SWNT)CCl₂ (**2b**) heated at 300 and 450 °C for 90 min, respectively.

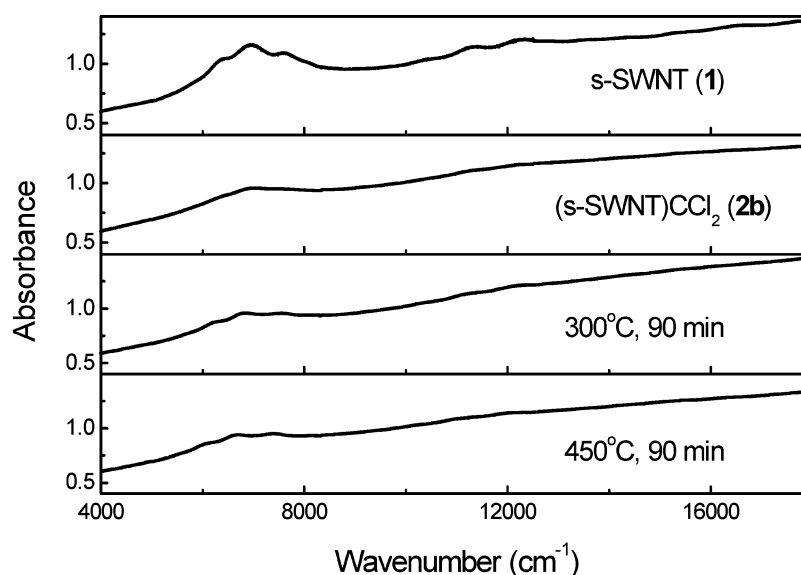


Figure 9. NIR spectra (film on Zn–Se substrate) of s-SWNT (**1**); (s-SWNT)CCl₂ (**2b**); and (s-SWNT)CCl₂ (**2b**) heated at 300 and 450 °C for 90 min, respectively.

to estimate the strength of the SWNT absorptions. The S_{11} band was chosen in this case as it has the highest amplitude, but more importantly because it is the most distinct spectral feature observable in the NIR spectra of HiPco SWNTs. Table 1 lists the $AA(S, X)/AA(T, X)$ ratio of the integrated area under the S_{11} spectral region (spectral cutoffs of $SCL = 5400$ and $SCH = 10\,750\text{ cm}^{-1}$), in which $AA(T, X)$ is the total area of SWNT absorption (sample number X) within this spectral range, and $AA(S, X)$ is the area under the S_{11} absorption after baseline correction (note the change in notation from the initial work,³³ where the areal absorption was previously denoted by A).³³ To estimate the effects of functionalization on the electronic structure, the absorption ratio is normalized by reference to the starting material s-SWNT (**1**). It was found that the $AA(S, X)/AA(T, X)$ value of (s-SWNT)CCl₂ (**2**) drops dramatically with an increasing degree of dichlorocarbene functionalization. This decrease in the absorption ratio clearly indicates that wall-functionalization serves to reduce the oscillator strength of the

interband transitions by introducing defects into the periodic band electronic structure of the SWNTs.

To further explore the relationship between the change in electronic structure of the s-SWNT (**1**) and the degree of dichlorocarbene functionalization, we calculated the relative intensity of the first semiconducting transition at constant SWNT concentration. Figure 4 shows the NIR spectra of s-SWNT (**1**) and (s-SWNT)CCl₂ (**2**) in dichlorobenzene, with the absorbance normalized to a common value at 8910 cm^{-1} (1.1 eV). A plot of the intensity of the first semiconducting transition (7000 cm^{-1}) in the functionalized SWNTs versus the degree of dichlorocarbene functionalization is shown as an inset to Figure 4. If the relationship between the degree of dichlorocarbene functionalization and the strength of interband transition is linear, the degree of functionalization necessary to remove all of the oscillator strength from this transition and to completely disrupt the band electronic structure of the SWNTs is estimated to be about 25%.

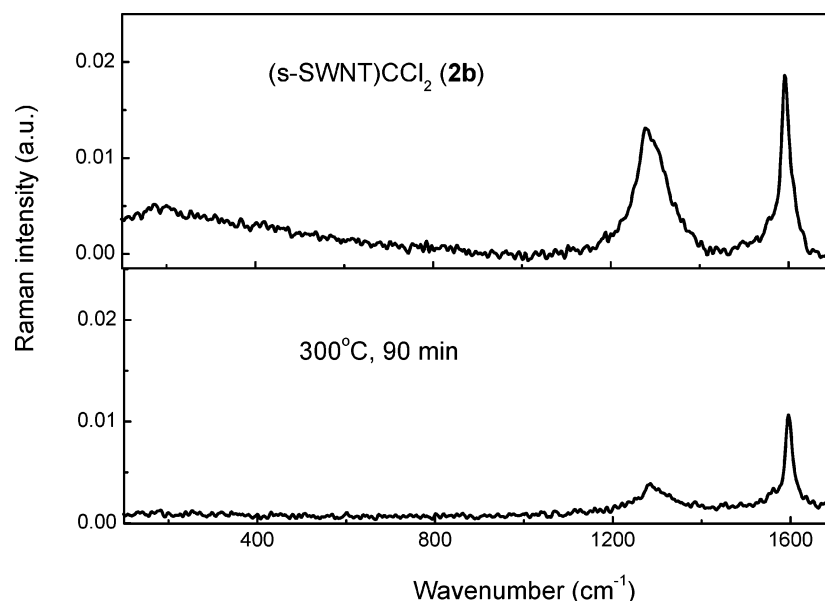


Figure 10. Raman spectra (film on Zn–Se substrate) of (s-SWNT) CCl₂ (**2b**) and (s-SWNT)CCl₂ (**2b**) heated at 300 °C for 90 min.

FIR Spectroscopy of SWNT Dichlorocarbene Reaction Products and Bromine-Doped SWNTs. In the foregoing discussion of the interband transitions of the covalent SWNT reaction products, we have focused on the NIR part of the spectrum, which involves electronic transitions between the occupied valence bands and the empty conduction bands of the SWNTs. However, the transitions occurring within partially filled energy bands involve the metallic electrons at the Fermi level, and this part of the spectrum should be extremely sensitive to sidewall chemistry. We have shown that ionic chemistry (doping) with electron acceptors introduced holes into the valence band of carbon nanotubes, thereby decreasing the intensity of the S₁₁ transition of the semiconducting SWNTs.^{2,31} However, ionic chemistry is not expected to destroy the periodicity of the SWNT lattice that is necessary for the preservation of the SWNT band structure, due to the weak localization effects of the counterions. Hence, ionic chemistry, where the electronic transitions disappear sequentially in order of increasing energy, is expected to differ substantially from covalent chemistry which introduces saturated bonds that function as defect sites in the extended π -network and eventually destroys the electronic band structure altogether. This weakens the strength of all of the interband transitions in both the semiconducting and the metallic SWNTs.^{2,4}

Figure 6 shows the IR–vis–UV spectra of films of s-SWNT (**1**) and (s-SWNT)CCl₂ (**2**), where it may be seen that the s-SWNTs (**1**) have the very strong FIR absorption expected for a metal (M₀ transition). However, because dichlorocarbene addition introduces saturated C–C single bonds in place of the π -bonds, oscillator strength is rapidly lost from the FIR band on functionalization, showing the sensitivity of the metallic properties to the introduction of defects.^{34,36} (s-SWNT)CCl₂ (**2a**), which has a degree of dichlorocarbene functionalization of 12%, shows a significant decrease in the intensity in the FIR absorption. For (s-SWNT)CCl₂ (**2b**), the 16% degree of dichlorocarbene functionalization removes over 90% of the FIR intensity. The results confirm that the formation of carbon–

carbon bonds to the sidewalls of the metallic SWNTs rapidly opens a gap at the Fermi level, changing a metal into a semiconductor by introduction of defect sites. The degree of functionalization to completely disrupt the band electronic structure of the SWNTs is estimated to be about 22% from the FIR data (inset to Figure 6), in good agreement with the estimate based on the NIR results (Figure 4).

To provide a point of comparison with the covalent chemistry described above, we examined the spectroscopic effects of bromine doping of SWNTs.^{37,38} As may be seen in Figure 7, treatment of the s-SWNT (**1**) with bromine leads to an enhancement in the Fermi level absorptions that are visible in the FIR due to metallic intraband transitions (S₁) that occur within the valence band of the semiconducting SWNTs as a result of the hole doping of this band. Thus, the FIR spectroscopy of the functionalized SWNTs provides a clear differentiation between the covalent sidewall chemistry of dichlorocarbene addition (reduction in FIR intensity) and the ionic chemistry that occurs upon bromine doping (increase in FIR intensity).

Thermal Treatment of SWNT Dichlorocarbene Reaction Products. We also studied the thermal stability of the (s-SWNT)CCl₂ (**2**), because this material offers the possibility of preparing cross-linked SWNTs.

Thin films were prepared by dissolving samples of (s-SWNT)CCl₂ (**2b**) in THF by sonication, and then spraying the dispersion onto zinc–selenium substrates. The films were heated under vacuum for 90 min.

A comparison of the mid-IR spectra of as-prepared and thermally annealed (s-SWNT)CCl₂ (**2b**) is shown in Figure 8. After (s-SWNT)CCl₂ (**2b**) was heated at 300 °C, the strength of the C–Cl stretch at 798 cm^{−1} is drastically reduced. This indicated that most of the C–Cl bonds are broken by the thermal treatment. The peaks at 2920 and 1663 cm^{−1} were also decreased by thermal treatment due to the removal of the long chain amide functionalities at the ends of SWNTs. When the (s-SWNT)-

(36) Minot, E. D.; Yaish, Y.; Sazonova, V.; Park, J.-Y.; Brink, M.; McEuen, P. L. *Phys. Rev. Lett.* **2003**, *90*, 156401-1–156401-4.

(37) Lee, R. S.; Kim, H. J.; Fischer, J. E.; Thess, A.; Smalley, R. E. *Nature* **1997**, *388*, 255–257.

(38) Rao, A. M.; Eklund, P. C.; Bandow, S.; Thess, A.; Smalley, R. E. *Nature* **1997**, *388*, 257–259.

CCl_2 (**2b**) sample was heated at 450 °C, the peak at 798 cm^{-1} almost completely disappeared, indicating that the removal of chlorine was virtually complete.

NIR spectra of the films (Figure 9) show that thermal treatment with concomitant removal of the chlorine does not lead to a recovery of the pristine spectrum. Furthermore, there is a shift of the absorption peak of (s-SWNT) CCl_2 (**2b**) to low energy. This may be due to damage of the carbon nanotubes and the generation of defects. We have previously reported that thermal cycling under vacuum can dedope acid-purified carbon nanotubes and that this leads to an increase in the intensity of the S_{11} SWNT absorption in the NIR spectra.³¹ Because no difference in the absorption intensity between heated and unheated (s-SWNT) CCl_2 (**2b**) films was found, we can further conclude that the changes in the absorption spectrum of (s-SWNT) CCl_2 (**2b**) as compared to s-SWNT (**1**) are not due to (ionic) doping, but due to the effect of covalent binding of the dichlorocarbene moiety to the s-SWNT. This addition cannot be reversed by thermal treatment to recover the perfectly conjugated wall structure of the SWNTs. With the release of chlorine during thermal treatment, the carbon from the adduct may rearrange within the sidewall of the SWNTs, or even dimerize to produce cross-linked SWNTs as observed in the heating of $\text{C}_{60}\text{CBr}_2$.¹⁶

Figure 10 shows the Raman spectra of the (s-SWNT) CCl_2 (**2b**) film before and after thermal treatment at 300 °C. The intensity of the disorder peak (ω_d) decreases after heating, which

suggests that some of the sp^3 hybridized carbons on the sidewall have been converted back into sp^2 carbons.

Conclusion

The decomposition of $\text{PhHgCCl}_2\text{Br}$ in solutions of soluble HiPco SWNTs leads to the addition of dichlorocarbene to the sidewalls of the carbon nanotubes. The strength of the interband electronic transitions of (s-SWNT) CCl_2 is suppressed as a result of the presence of sp^3 hybridized carbon atoms within the sidewalls of the SWNTs. The effects on the electronic transitions at the Fermi level are particularly dramatic as the dichlorocarbene addition converts metallic SWNTs to semiconducting SWNTs, and this covalent chemistry offers a sharp contrast with the enhanced absorption in the FIR that is observed with ionic chemistry. Thermal treatment of samples of (s-SWNT) CCl_2 above 300 °C resulted in the breakage of the C–Cl bonds, but the electronic structure of the SWNTs was not recovered.

Acknowledgment. This work was supported by the MRSEC Program of the National Science Foundation under Award No. DMR-9809686 and by DOD/DARPA/DMEA under Award No. DMEA90-02-2-0216.

Note Added after ASAP: The version published on the Web 11/11/2003 contained minor errors in the labels and captions to Figures 5–7. The final Web version published 11/13/2003 and the print version are correct.

JA0356737